Determining the daytime Earth's shortwave fluxes from DSCOVR

Wenying Su (Wenying.Su-1@nasa.gov)
NASA Langley Research Center, Hampton, VA

L. Liang, D. P. Duda, P. Minnis, K. Khlopenkov, M. K. Thiemann
SSAI, Hampton, VA

Publications

1. Wenying Su, L. Liang, D. P. Duda, K. V. Khlopenkov, M. Thieman, Global daytime mean shortwave flux consistency under varying EPIC viewing geometries, *Frontiers Remote Sens.,* accepted, 2021.
2. Conor Haney, David Doelling, Wenying Su, Rajendra Bhatt, Arun Gopalan and Benjamin Scarino, Radiometric Stability Assessment of the DSCOVR EPIC Visible Bands using MODIS, VIIRS, and Invariant Targets as Independent References, Frontiers Remote Sens. , under revision, 2021.
3. Andrew A Lacis, Barbara E Carlson, Gary L Russell, Alexander Marshak and Wenying Su, NISTAR and EPIC Inspired Climate GCM Diagnostics of the Earth's Planetary Albedo and Cloud Distribution via Longitudinal Data Slicing, Frontiers Remote Sens. , submitted, 2021.
4. Valero, F. P. J., A. Marshak, and P. Minnis, LaGrange point missions: The key to next generation integrated Earth observations. DSCOVR innovation. *Frontiers Remote Sens.*, doi:10.3389/frsen.2021.745938, 2021.
5. Daniel R. Feldman, Wenying Su, Pat Minnis, Subdiurnal to interannual frequency analysis of observed and modeled reflected shortwave radiation from Earth, 48, e2020GL089221, 10.1029/2020GL089221, Geophysical Research Letter, 2021.
6. Wenying Su, P. Minnis, L. Liang, D. P. Duda, K. V. Khlopenkov, M. Thieman, Y. Yu, A. Smith, S. Lorentz, D. Feldman, F. P. J. Valero, Determining the daytime Earth radiative flux from National Institute of Standards and Technology Advanced Radiometer (NISTAR) Measurements, 13, 429-443, Atmos. Meas. Tech., 10.5194/amt-13-429-2020, 2020.
7. Barbara Carlson, Andrew Lacis, Christopher Colose, Alexander Marshak, Wenying Su, Steven Lorentz, Spectral signature of the biosphere: NISTAR finds it in our solar system, Geophys. Res. Lett., 10.1029/2019GL083736, 2019.
8. Doelling, D., Haney, C., Bhatt, R., Scarino, B., and Gopalan, A. (2019). The Inter-Calibration of the DSCOVR EPIC Imager with Aqua-MODIS and NPP-VIIRS. Remote Sens. 11, 1609. doi:10.3390/rs11131609
9. Yang, Y., Meyer, K., Wind, G., Zhou, Y., Marshak, A., Platnick, S., Min, Q., Davis, A. B., Joiner, J., Vasilkov, A., Duda, D., and Su, W.: Cloud Products from the Earth Polychromatic Imaging Camera (EPIC): Algorithms and Initial Evaluation, Atmos. Meas. Tech., 12, 2019-2031, https://doi.org/10.5194/amt-12-2019-2019, 2019.
10. Wenying Su, L. Liang, D. R. Doelling, P. Minnis, D. Duda, K. Khlopenkov, M. Thieman, N. G. Loeb, S. Kato, F. P. J. Valero, H. Wang, and F. Rose. Determining the shortwave radiative flux from earth polychromatic imaging camera. J. Geophys. Res., 123, doi:10.1029/2018JD029390, 2018.
11. K. khlopenkov, D. Duda, M. Thieman, P. Minnis, W. Su, and K. Bedka. Development of multi-sensor global cloud and radiance composites for Earth radiation budget monitoring from DSCOVR, Remote sensing of clouds and the atmosphere XXII, Editors: E. I. Kassianov, K. Schafer, R. H. Picard, and K. Weber, Volume 10424K. Proc. of SPIE, 2017.
12. C. O. Haney, D. R. Doelling, P. Minnis, R. Bhatt, B. Scarino, and A. Gopalan. The calibration of the DSCOVR EPIC multiple visible channel instrument using MODIS and VIIRS as a reference. In Proc. of SPIE, volume 9972, 2016.

Objectives of the project

- Produce global daytime mean fluxes from radiances observed by NISTAR and EPIC (Su et al., 2018, 2020, 2021)
  - Determine the global daytime mean SW and LW anisotropic factors (Su et al., 2018)
  - Use EPIC cloud composite data for scene identification (Khlopenkov et al., 2017), and for evaluating EPIC cloud product (Yang et al., 2019)
- Evaluate the global climate models using the high-temporal-resolution fluxes (Carlson et al., 2019, Feldman et al., 2021, Lacis et al., 2021)
- Calibrate EPIC visible channels using MODIS, VIIRS, and invariant targets (Doelling et al., 2019, Haney et al., 2016, 2021)

Global daytime mean radiances from NISTAR and EPIC

- NISTAR provides continuous broadband radiance measurements for the shortwave and total channels from the sunlit side of the Earth as a single pixel.
- EPIC provides 10 narrow band spectral images of the entire sunlit side of the Earth using a 2048x2048 pixel CCD (Charge Coupled Device) detector.
  - Use the EPIC narrowband channels of blue, green, and red to derive the shortwave (SW) broadband reflectance (Su et al., 2018).
  - Narrowband to broadband (NB2BB) regression coefficients are developed based upon collocated MODIS and CERES data for all-sky conditions separately for ocean and non-ocean surfaces using corresponding MODIS channels.
  - Apply these relationships to EPIC 443, 551, and 680nm channels to derive EPIC broadband radiance (I^{bb}_e) for <u>each pixel</u>.
  - EPIC pixel-level broadband SW radiances are averaged to calculate the <u>global daytime mean s</u>hortwave radiance.

Radiances depend on the EPIC viewing geometry

- DSCOVR's elliptical Lissajous orbit is a quasi-periodic orbit and its distance and viewing geometries change from day to day.
- From January 2017 to June 2019, the relative azimuth angles show small month-to-month variations and the maximum value does not exceed 175°. However, the relative azimuth angles of 2020 show large month-to-month changes with the maximum relative azimuth angle exceeding 178° in December.

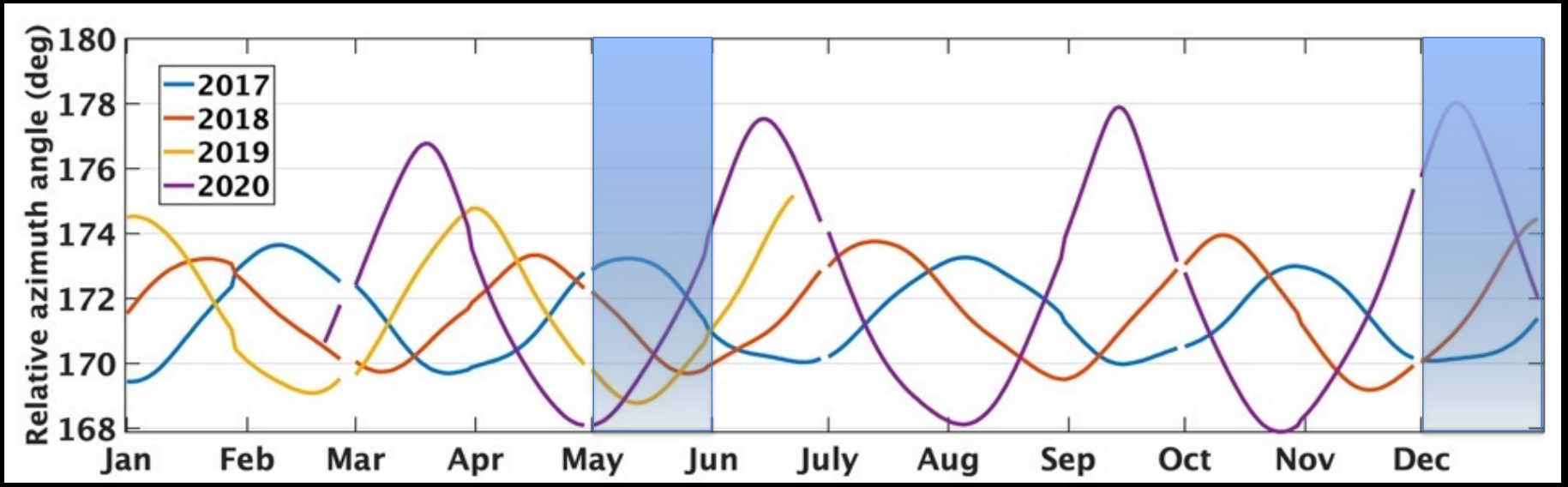

Radiance increases as relative azimuth angle increases

May

December

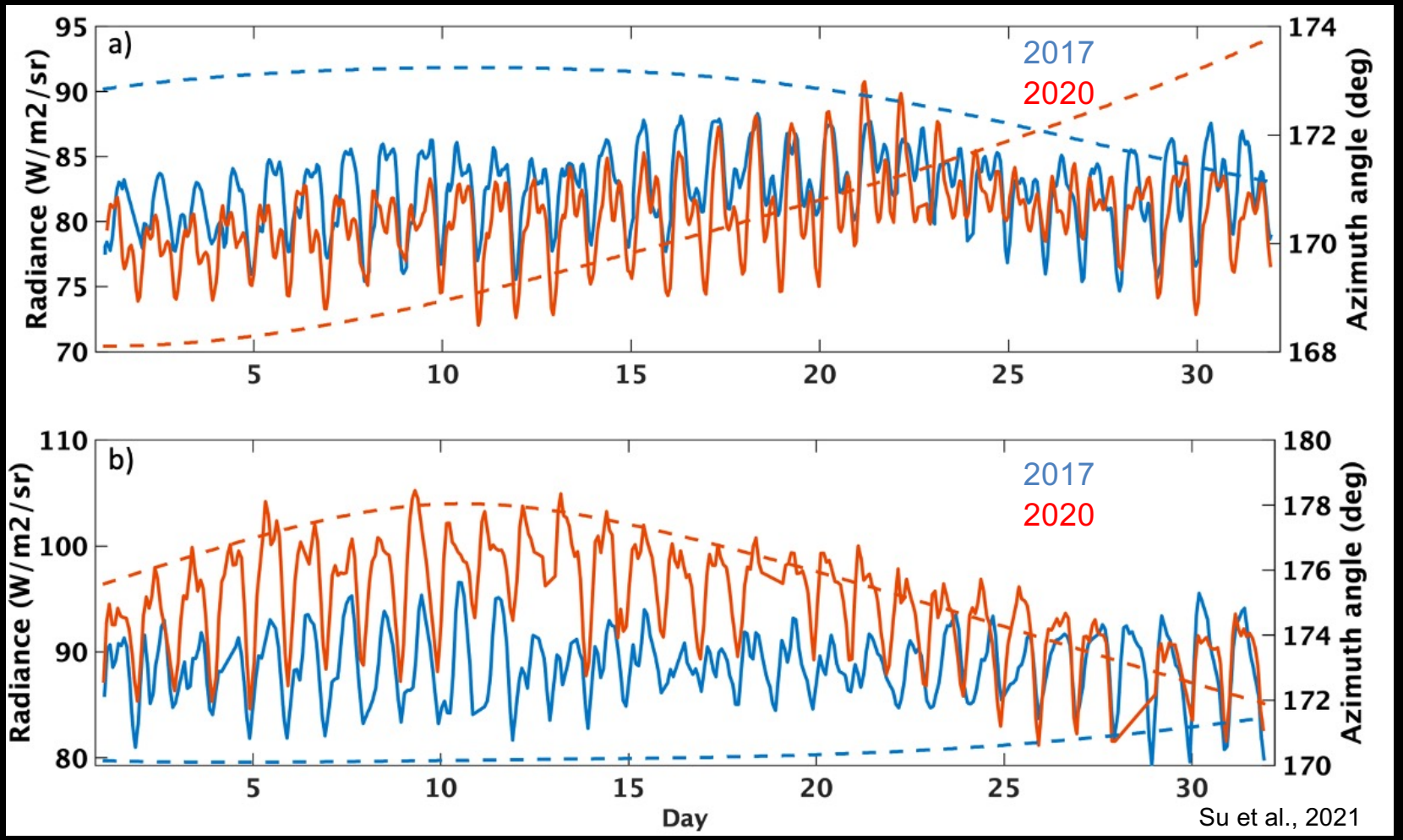

Su et al., 2021

Anisotropy of the TOA radiance field must be considered when converting radiances to fluxes

$$F(\theta_0) = \frac{\pi I_o(\theta_0, \theta, \phi)}{R(\theta_0, \theta, \phi)}$$

- Using the scene-type dependent CERES empirical angular distribution models (ADMs, Su et al. 2015);
- Scene type is defined based upon many variables: surface type, cloud fraction, cloud optical depth, cloud phase, wind speed, etc.;
- Low spatial resolution of EPIC imagery (20x20 km^2) and its lack of infrared channels diminish its capability to identify clouds and to accurately retrieve cloud properties;
- To determine the scene type for each EPIC pixel, we take advantage of the cloud property retrievals (Minnis et al. 2008, 2021) from multiple imagers on low Earth orbit (LEO) satellites and on geostationary (GEO) satellites;
- Cloud property retrievals from these LEO/GEO imagers are optimally merged together to provide a seamless global composite product at 5-km resolution.

Global composite data are then remapped into the EPIC field of view by convolving the high-resolution cloud properties with the EPIC point spread function to produce the EPIC composite: an example of 11:15 UTC, 4 Jan. 2017

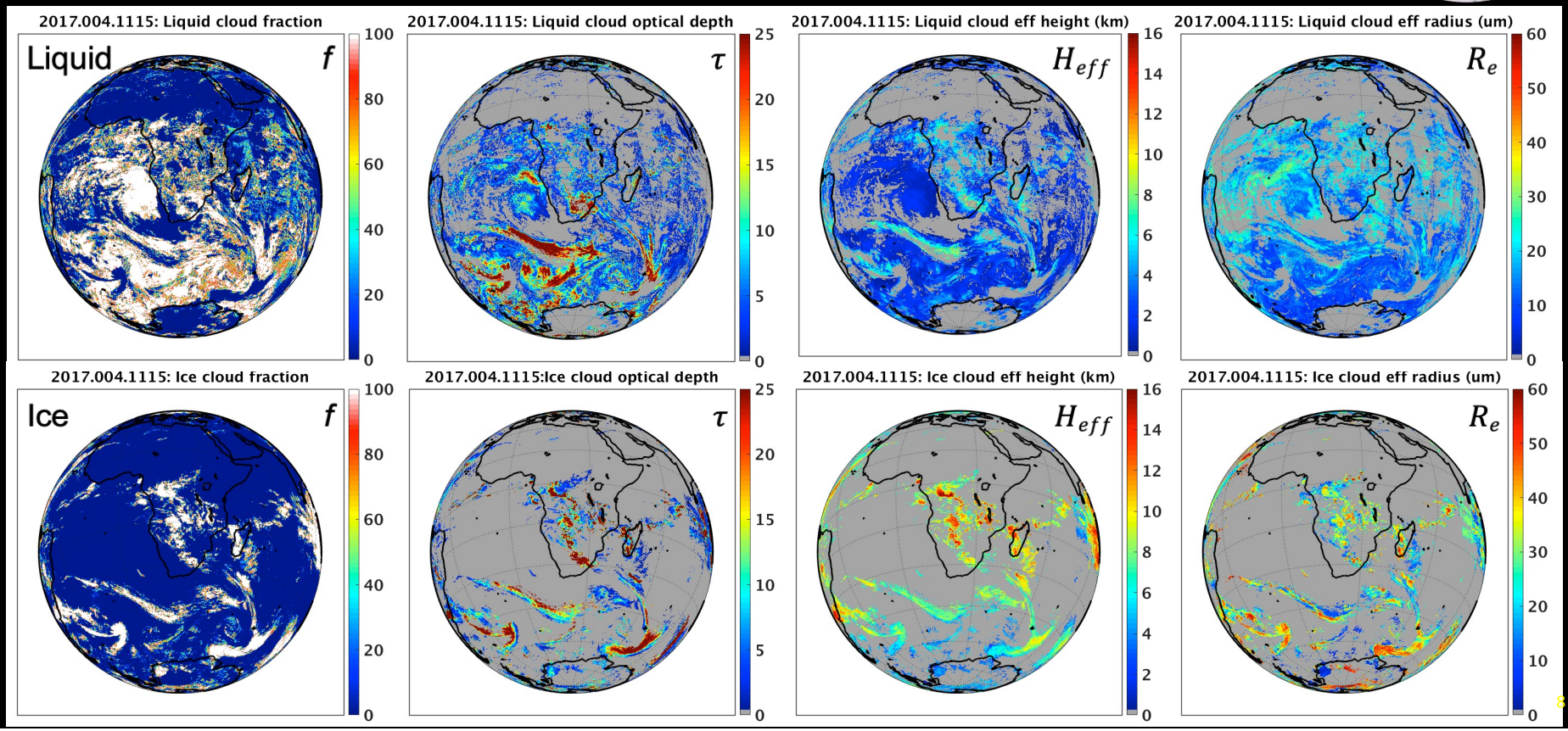

Global daytime mean cloud fractions differ little between 2017 and 2020

May

December

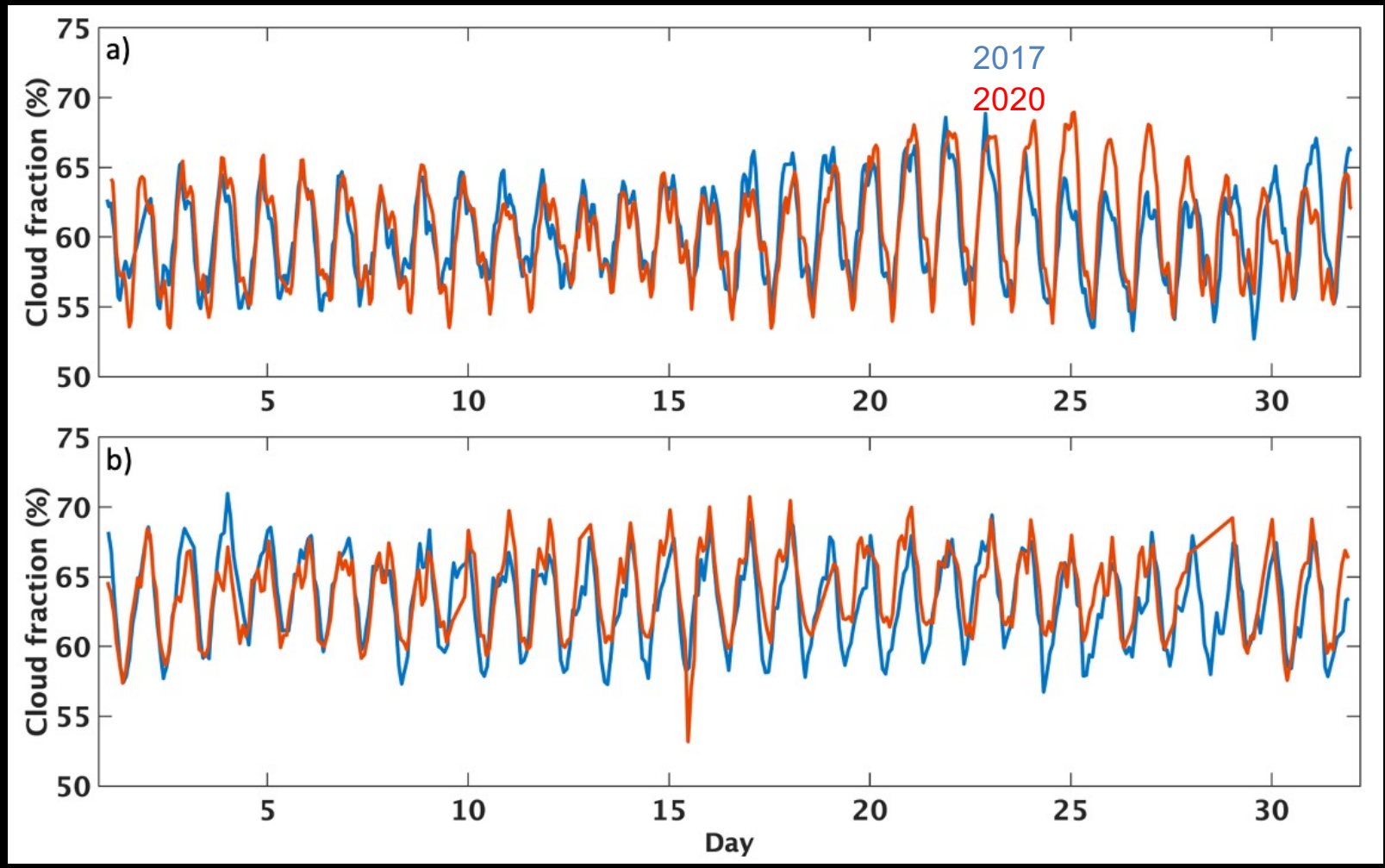

Global mean anisotropic factors increase as the EPIC relative azimuth angles move closer to backscattering direction

- The EPIC relative azimuth angle is 170° for December 5, 2017, and it is 177° for December 5, 2020.
- The SW anisotropic factors for the two UTC times are:
  - 2017: 1.241/1.254
  - 2020: 1.343,/1.375

2017

2020

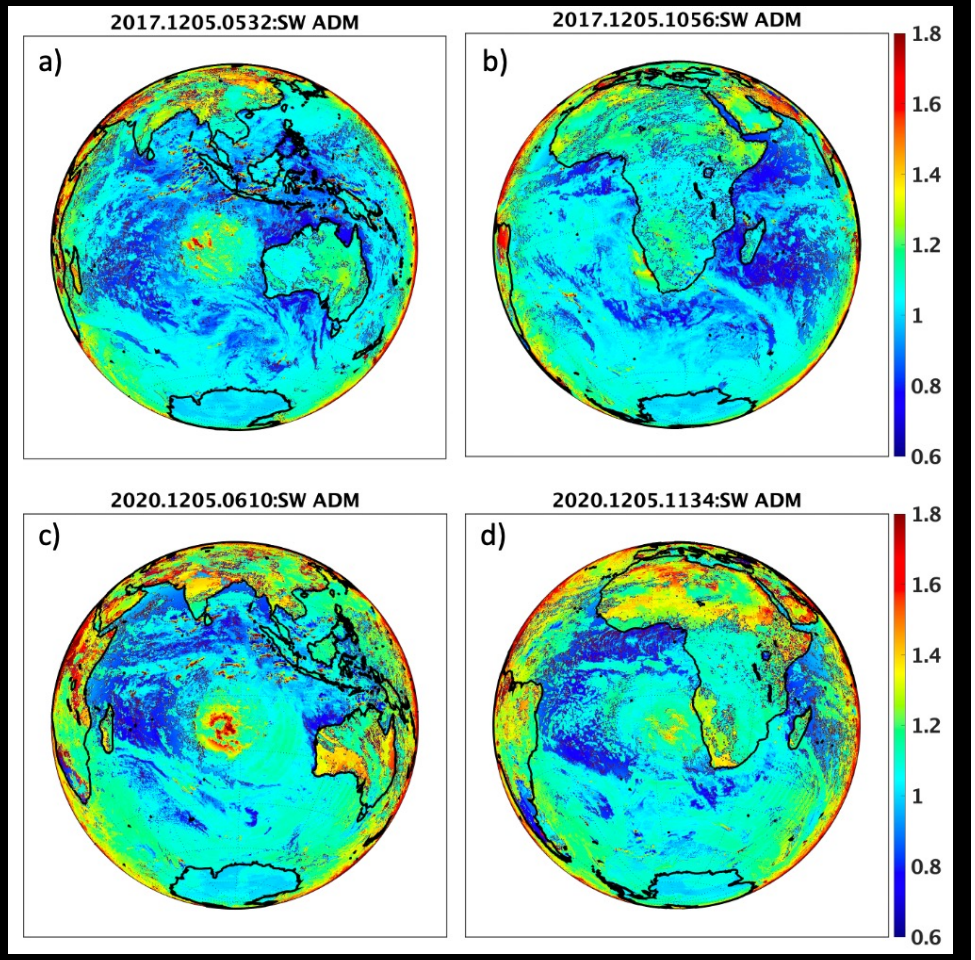

Anisotropic factors change as relative azimuth angles

- The clear cropland anisotropy factor increases by up to 30% around θ = 40° (the hot sport) when the relative azimuth angle moves from 170° to 179°.
- Anisotropy factor for liquid clouds increases by up to 9% around the glory (θ = 60°) when the relative azimuth angle moves from 170° to 179°.

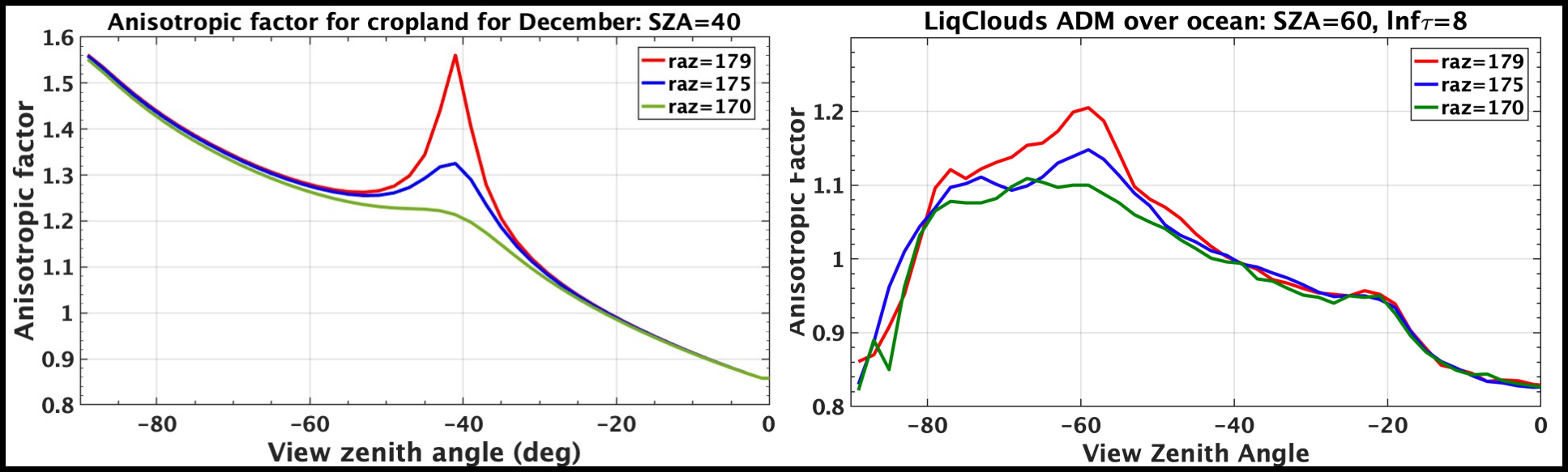

SW flux differences between 2017 and 2020 are much smaller than SW radiance differences

May

December

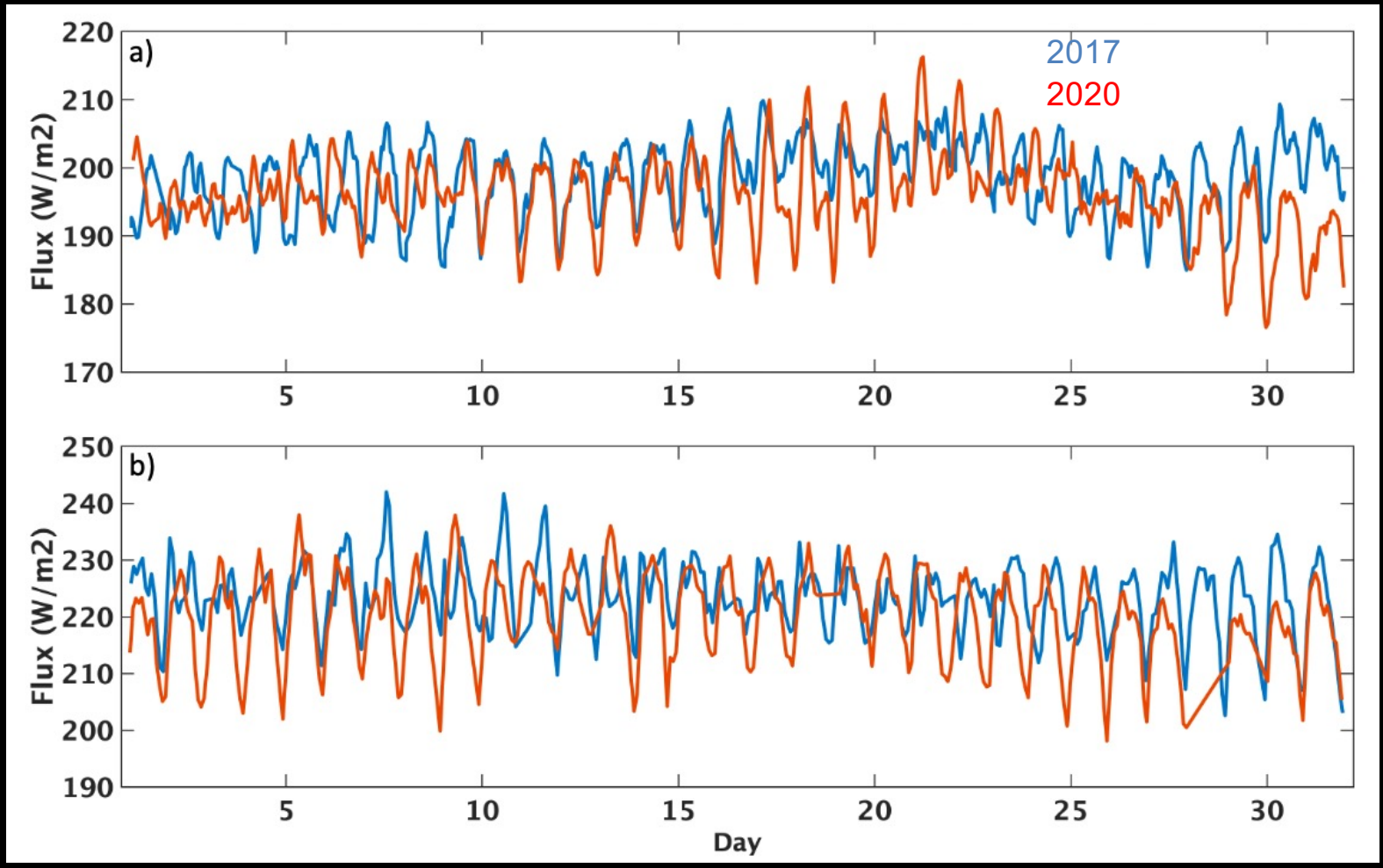

Comparison between EPIC and CERES SYN fluxes

Daytime SW flux from CERES SYN

EPIC view mask:
Red: Daytime areas within EPIC view
Grey: Nighttime areas within EPIC view
Blue line: terminator boundary

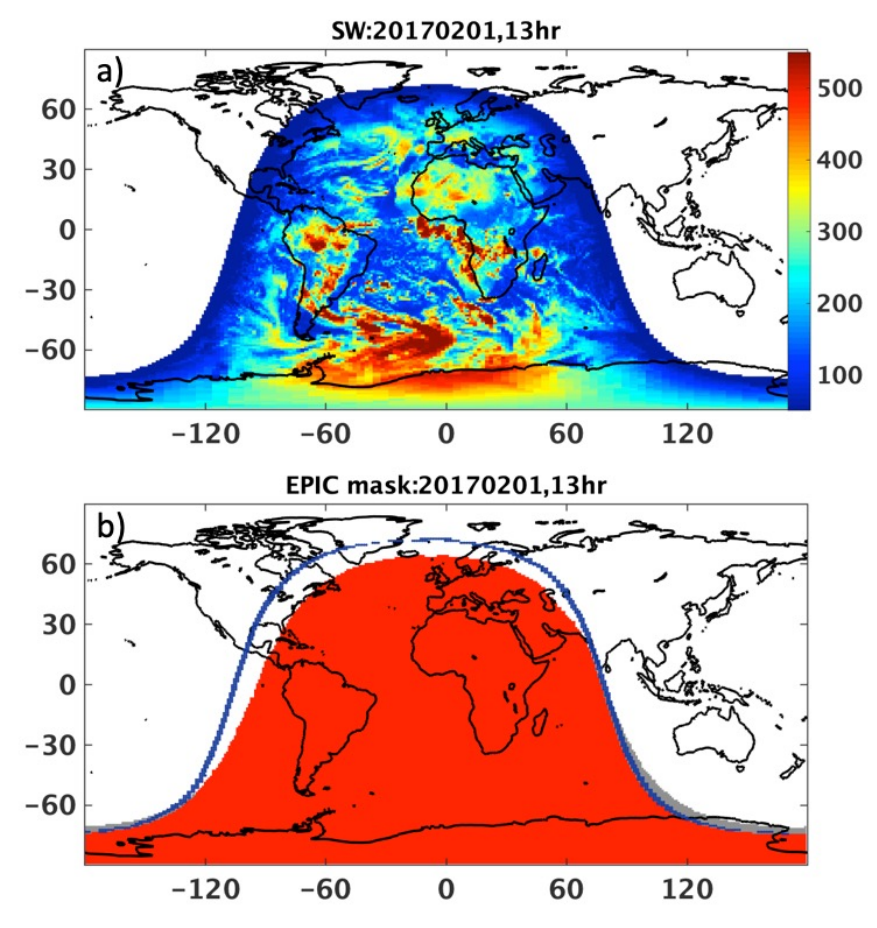

- CERES synoptic product (SYN) also provides hourly TOA SW and LW fluxes;
- To compare the hourly SYN data with EPIC flux, only consider the daytime SYN grid boxes that are visible to EPIC, and these data are weighted by cos(latitude):

$$\overline{F_{syn}} = \frac{\sum F_j cos(lat_j)\omega_j}{\sum cos(lat_j)\omega_j}$$

Comparison between EPIC and CERES SW fluxes for May and December

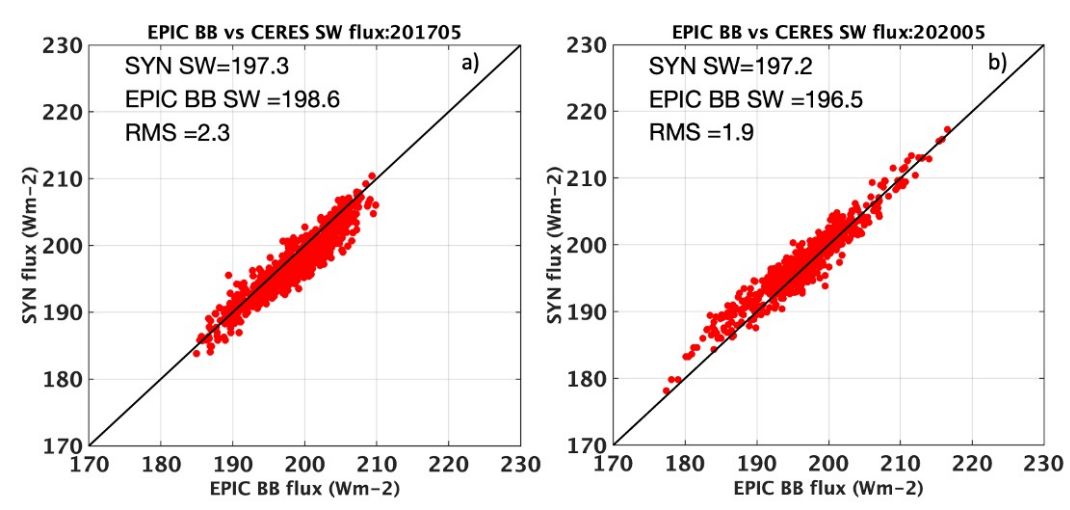

May

December

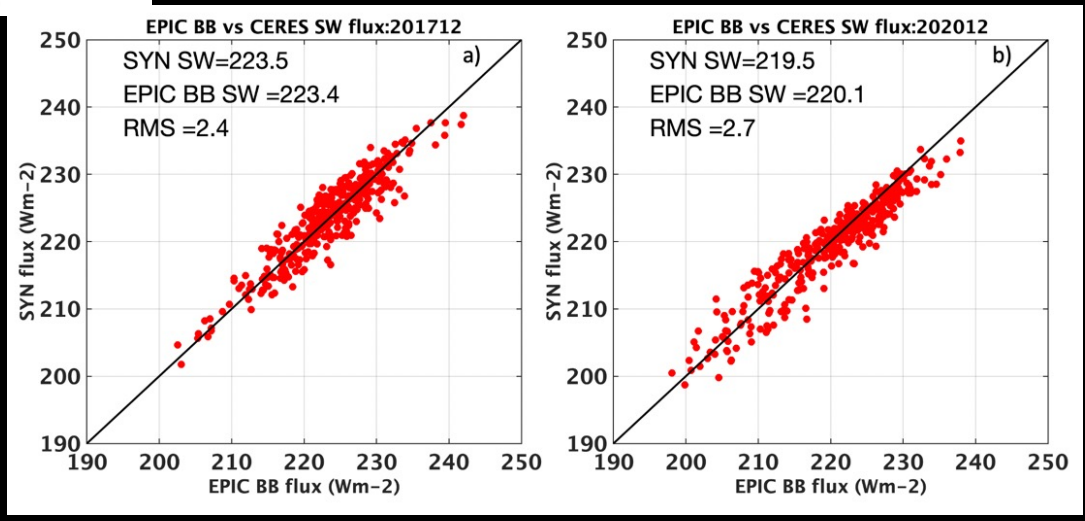

Global daytime SW flux comparison between CERES and EPIC

Hourly gridded CERES synoptic (SYN) SW fluxes are integrated over the areas that are visible to EPIC/NISTAR.

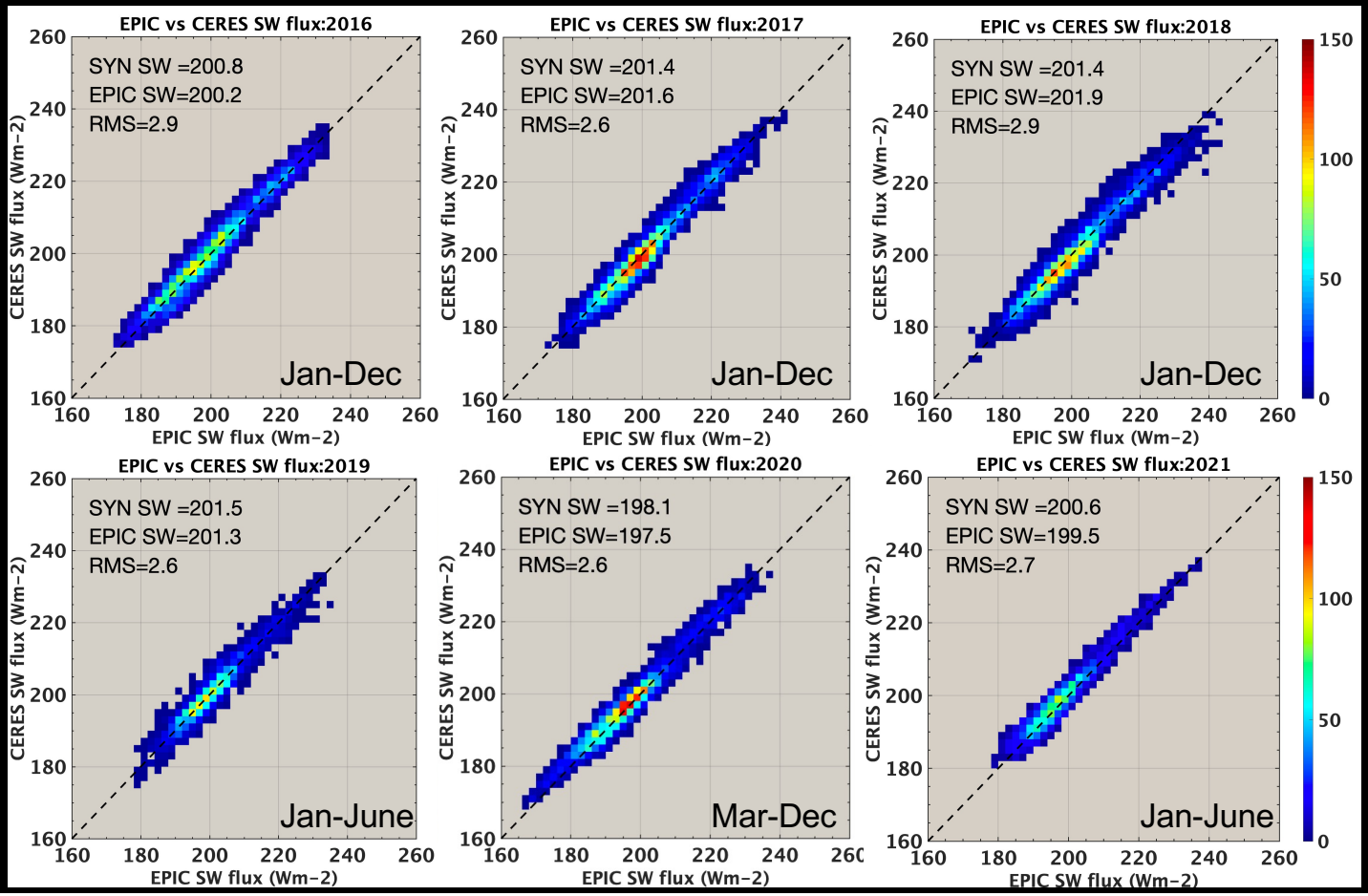

Monthly daytime mean SW fluxes from EPIC and CERES

- Multi-year mean EPIC SW flux is 202.3 Wm-2
- Multi-year mean CERES SYN SW flux is 202.8 Wm-2
- RMS error is 1.3 Wm-2

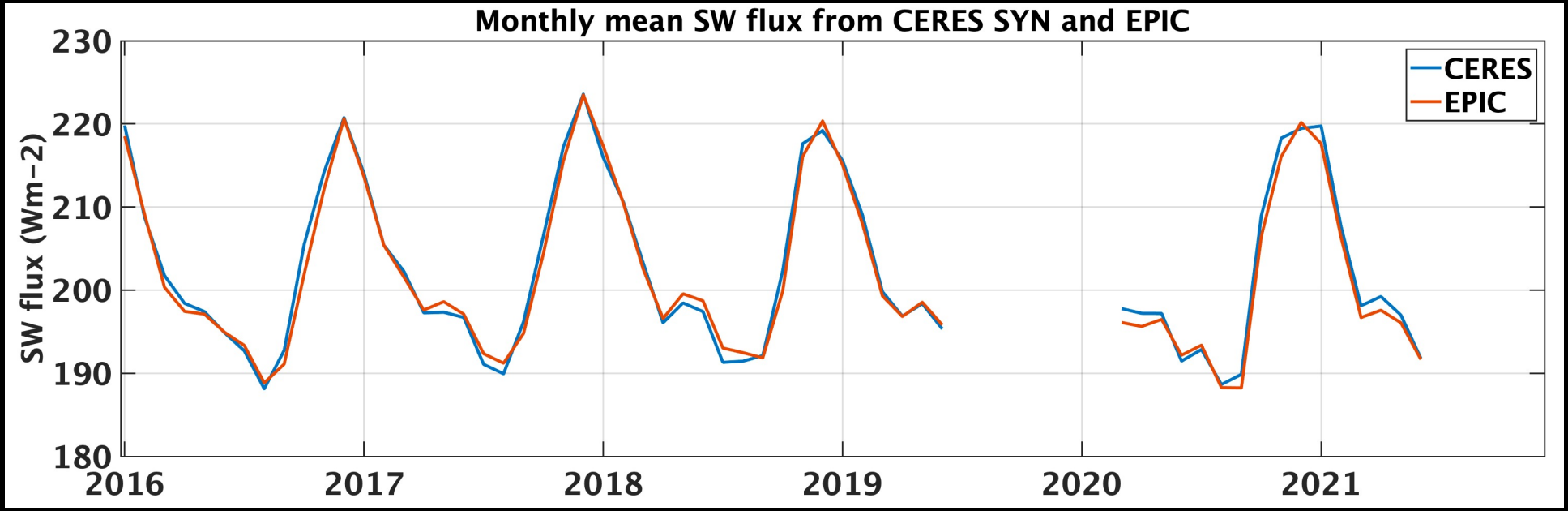

Summary

- Produced EPIC cloud composite and EPIC SW flux from January 2016 to June 2021.
- EPIC SW fluxes agree very well with CERES SYN SW fluxes, despite the viewing geometries of EPIC differ significantly from CERES.
- CERES angular distribution models capture the anisotropy changes for relative azimuth angles between 168° to 178°.